Neutron background estimates in the tagger hall

A. Somov, *JLAB.*

Abstract

This note describes the simulation of the neutron background in the microscope detector region of the tagger hall. The background was estimated for various layouts of the vacuum chamber and sizes of the electron beam pipe.

1 Introduction

In the original design of the tagger microscope detector, the microscope was planned to be instrumented with SiPMs photo-detectors for detecting light from scintillating fibers. Radiation tests recently carried out at JLab indicated large sensitivity of these photo-detectors to neutron radiation [1]. Specifically, irradiation of a $2 \times 2\ mm^2$ Photonic SiPM with a neutron source leads to the increase of a dark current of the detector by about a factor of 5 for the accumulated neutron dose of 50 rems. In order to estimate the degradation of the microscope SiPM performance caused by the neutron radiation, we have performed a detailed simulation of the neutron background in the tagger hall using a Geant program provided by the JLab Radiation Control (RadCon) group [2]. The RadCon Geant includes a better description of the photo/electro-nuclear processes than the standard Geant 3. We implemented the tagger hall and the electron beam dump geometries into the Geant simulation according to the latest technical drawing [3] and recent simulation of the single dipole tagger magnet [4]. The tagger hall geometry is presented in Fig. 1. The neutron dose was computed along the focal plane and at the position of the microscope counters.

Most of the background particles are expected to originate in interactions of scattered beam electrons with the downstream flange of the tagger magnet vacuum chamber and the electron beam pipe leading to the beam dump. In order to optimize designs of the vacuum chamber and the beam pipe, we computed doses for different chamber lengths and pipe widths.

According to the previous background studies performed by the radiation control group [5], the neutron background will be dominated by neutrons produced inside the

tagger hall directly, rather than inside the beam dump area. Detailed simulation of showers produced by a 12 GeV 2.2μA electron beam in the dump area requires a significant amount of CPU time. In the current analysis, we do not consider background originating from the electron beam dump, i.e., particles in Geant were stopped after the third (most downstream) labyrinth wall. Simulation of background induced by the beam dump area for the updated tagger hall geometry has to be performed in the future studies.

In the Geant simulation, 12 GeV pencil-beam electrons were incident on a 20 μm thick diamond crystal. The background was estimated assuming high luminosity corresponding to the electron beam current of 2.2 μA[1].

The neutron dose was computed in units of rem using biological damage coefficients presented in the top plot of Fig.3. The estimated dose can be compared with the radiation measurements of SiPMs using a neutron source. The shape of the biological damage coefficients curve is somewhat similar to that of the effective damage to Silicon detectors caused by neutrons. The latter curve, normalized to a damage of 1 MeV neutrons is shown in the bottom plot of Fig. 2.

2   Simulation Results

The downstream flange of the vacuum chamber and the electron beam pipe are considered to be one of the major sources of background in the focal plane. We studied neutron background for different radii of the electron beam pipe and lengths of the vacuum chamber. The chamber length was extended by moving the flange at the downstream end further away from the focal plane, as shown in Fig. 3. In the simulation, we used a round-shaped stainless steel electron beam pipe with the wall thickness of 1.5 mm. The pipe was positioned in such a way that the full-energy electrons were situated closer to the distant side of the pipe. The distance between the trajectory of the full-energy electrons and the pipe wall constituted 1 inch. Geometries, considered in the simulation are listed below:

1. **Short vacuum chamber, no pipe walls.** The downstream end of the vacuum chamber is shown in the upper plot of Fig. 3. The electron pipe had no walls, i.e., it was modeled as a 4 inch tube filled with vacuum.

2. **Short vacuum chamber, $4^{''}$ pipe.** The same vacuum chamber length as in (1). The electron beam pipe had a diameter of $4^{''}$.

3. **Short vacuum chamber, $6^{''}$ pipe.** The same length of the vacuum chamber as in (1). The beam pipe diameter was increased to $6^{''}$.

4. **Middle vacuum chamber, $6^{''}$ pipe.** The vacuum chamber length was increased by about 50 cm in the downstream direction, as shown in the middle plot of Fig. 3. The chamber was connected to a $6^{''}$ pipe.

---

[1]The angular direction of a bremsstrahlung electron after emitting a photon is not updated in Geant, which leads to the underestimation of the angular spread of scattered electrons. Therefore, the simulation represents a conservative estimate of the neutron background.

5. **Long vacuum chamber, $6''$ pipe.** The vacuum chamber length was further increased as presented in the bottom plot of Fig. 3. The chamber was followed by a $6''$ pipe.

6. **Long vacuum chamber, $6''$ pipe, shielded.** The same geometry as in (5). The microscope detector was surrounded by polyethylene walls in order to thermalize neutrons and consequently reduce the neutron dose. Geant volumes used for shielding are presented in Fig. 4.

Neutron doses averaged over the focal plane in the region $10\text{ cm} < |Y| < 50\text{ cm}$ and $415\text{ cm} < Z < 1259\text{ cm}$ are listed in the middle column of Table 1. The corresponding doses in the microscope detector region, defined as $750\text{ cm} < Z < 824\text{ cm}$ and $10\text{ cm} < |Y| < 50\text{ cm}$, are presented in the right column of Table 1. Due to the limited statistics in the microscope detector region for the geometry with the polyethylene shielding, the doses were averaged over the larger Y range: $10\text{ cm} < |Y| < 100\text{ cm}$. As expected, the neutron dose is getting smaller when the major particle scattering sources (the downstream flange of the VC and the electron beam pipe) move further away from the focal plane. The dose distribution along the focal plane for the long vacuum chamber and $6''$ beam pipe (geometry #5) is presented in the left plot of Fig. 5. The corresponding dose distribution along the Y axis in the microscope detector region is presented in the right plot of Fig. 5.

As follows from Table 1, the polyethylene shielding (geometry #6) reduces the neutron dose in the microscope detector region by about a factor of 6. The dose distribution along the Y axis for this geometry is presented in Fig. 6.

X-Z coordinates of the origin of neutrons that pass through the focal plane are presented in Fig. 7. About 41% of all background neutrons penetrating the microscope detector region originate in interactions of scattered electrons inside the dipole magnet and walls of the vacuum chamber[2]. For the geometry with the polyethylene shielding these neutrons contribute to about 56% of the total neutron dose.

Layout	Dose (mrem/h)	
	Focal plane	Microscope area
1. Short VC, vacuum pipe without walls	143	142
2. Short VC, 4 inch pipe	343	247
3. Short VC, 6 inch pipe	269	183
4. Middle VC, 6 inch pipe	215	187
5. Long VC, 6 inch pipe	199	182
6. Long VC, 6 inch pipe, shield		27

Table 1: Neutron doses averaged over the focal plane and the microscope region for various layouts of the vacuum chamber and the electron beam pipe.

---

[2]This number does not include neutrons produced at the downstream flange of the vacuum chamber.
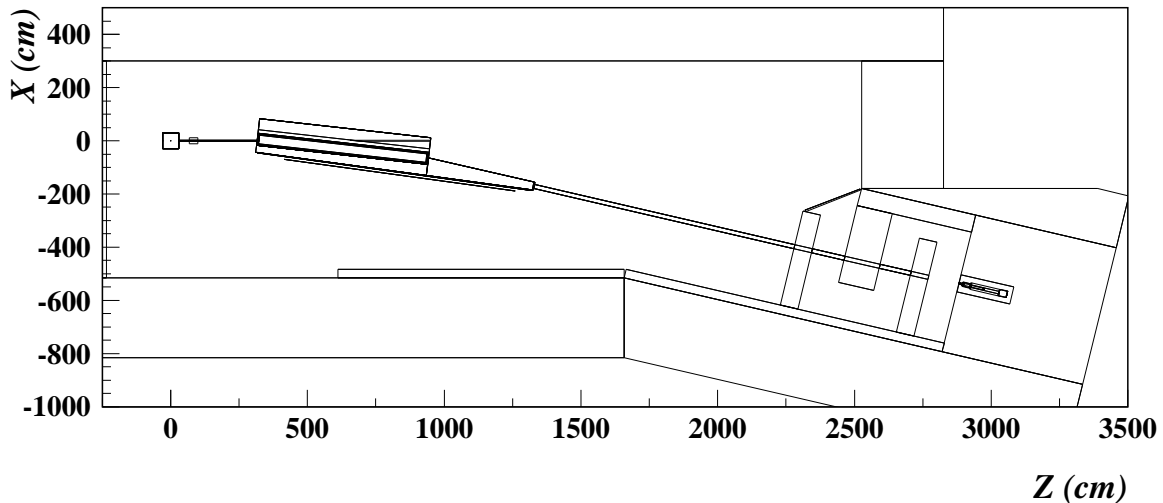
Figure 1: Elevation view of the tagger Hall geometry implemented in the Geant simulation.

3 Discussion

We observed a relatively large neutron background, on the level of about 200 mrem/h, in the microscope detector region. The neutron dose is expected to significantly increase the dark current of the SiPMs after a few days of operation. The neutron background was substantially reduced when the microscope detector region was surrounded by 10 cm thick shielding walls, but still remained at a relatively high level of about 30 mrem/h. According to the radiation test results, this dose will lead to the increase of the SiPM dark current by almost a factor of 5 after continuous running of the GlueX experiment for about 2.5 months. More than 50% of the neutron dose comes from neutrons produced inside the magnet and on walls of the vacuum chamber. The current simulation does not include possible contributions to the neutron background from the electron beam dump.

Further shielding of the microscope detector area from neutron radiation might be possible, but will require more technical efforts and detailed simulation studies. Consideration of an alternative or backup instrumentation of the microscope detectors is recommended.

4 Appendix

We subsequently estimated neutron background originating from the electron beam dump by passing 12 GeV pencil-beam electrons directly to the dump. The beam dump geometry and an example of the ineraction of the beam electron inside the dump is shown in Fig. 8. The neutron dose was computed for the long vacuum chamber and $6''$ electron beam pipe (layout #5 in Table 1) assuming running at high-luminosity, that corresponds to the

4

electron beam intensity of $\sim 1.4 \cdot 10^{13}$ e/s. The dose was averaged over the fixed-array detector region, defined as 415 cm $< Z <$ 1259 cm. Due to limited statistics, overaging in Y was performed between 10 cm $< |Y| <$ 100 cm. The neutron dose was estimated to be 39 mrem/h. The corresponding background induced by neutrons produced before the dump is about 200 mrem/h.

References

[1] Neutron radiation tests performed by Yi Qiang `hhttp://www.jlab.org/Hall-D/software/wiki/index.php/SiPM_Radiation_Hardness_Test`

[2] Modified Geant 3.21 with improved description of photon-nucleus interactions provided by Pavel Degtyarenko. The Geant and some Hall-D related geometries are located at tape /mss/home/somov/pavel1.tar.gz.

[3] HSMM drawings, Feb. 25, 2008.

[4] A. Somov, Resolution studies of a dipole tagger magnet: response to the magnet review referees, GlueX-doc-1386.

[5] Pavel Degtyarenko, private communications regarding simulation of the beam dump area.
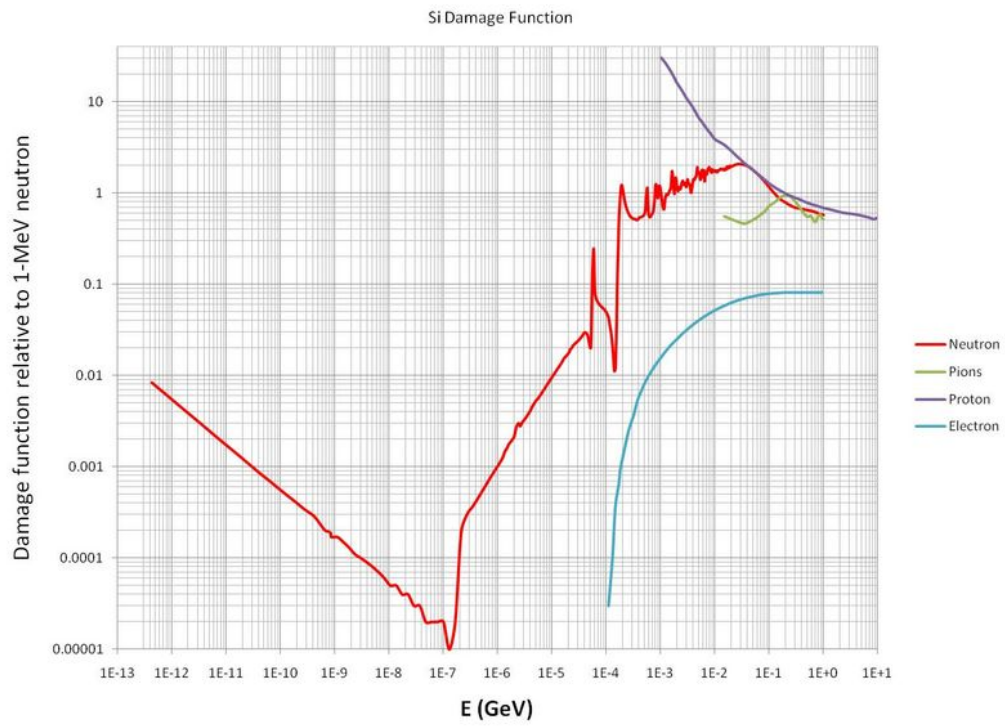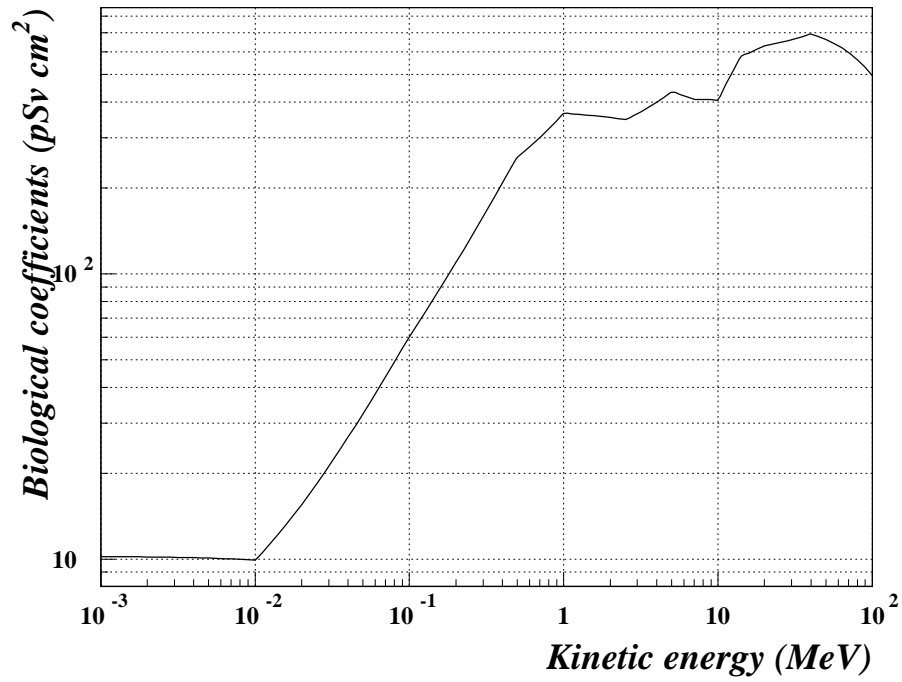
Figure 2: Biological damage conversion coefficients for neutrons (top). Effective damage to Silicon detector relative to 1 MeV neutron (bottom).
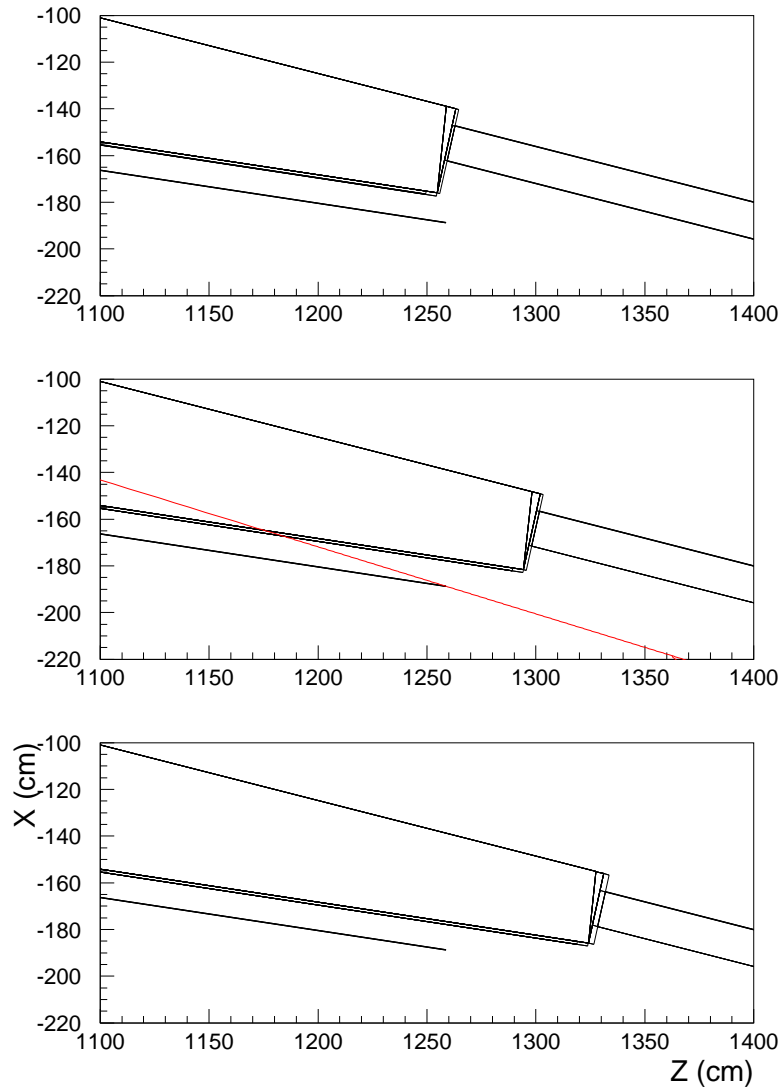
Figure 3: Three geometries of the downstream end of the vacuum chamber studied with the Geant simulation. The vacuum chamber is followed by the electron beam pipe leading to the beam dump. The solid curve in front of the vacuum chamber represents the focal plane. The dashed curve in the middle plot shows the trajectory of a 9 GeV electron.
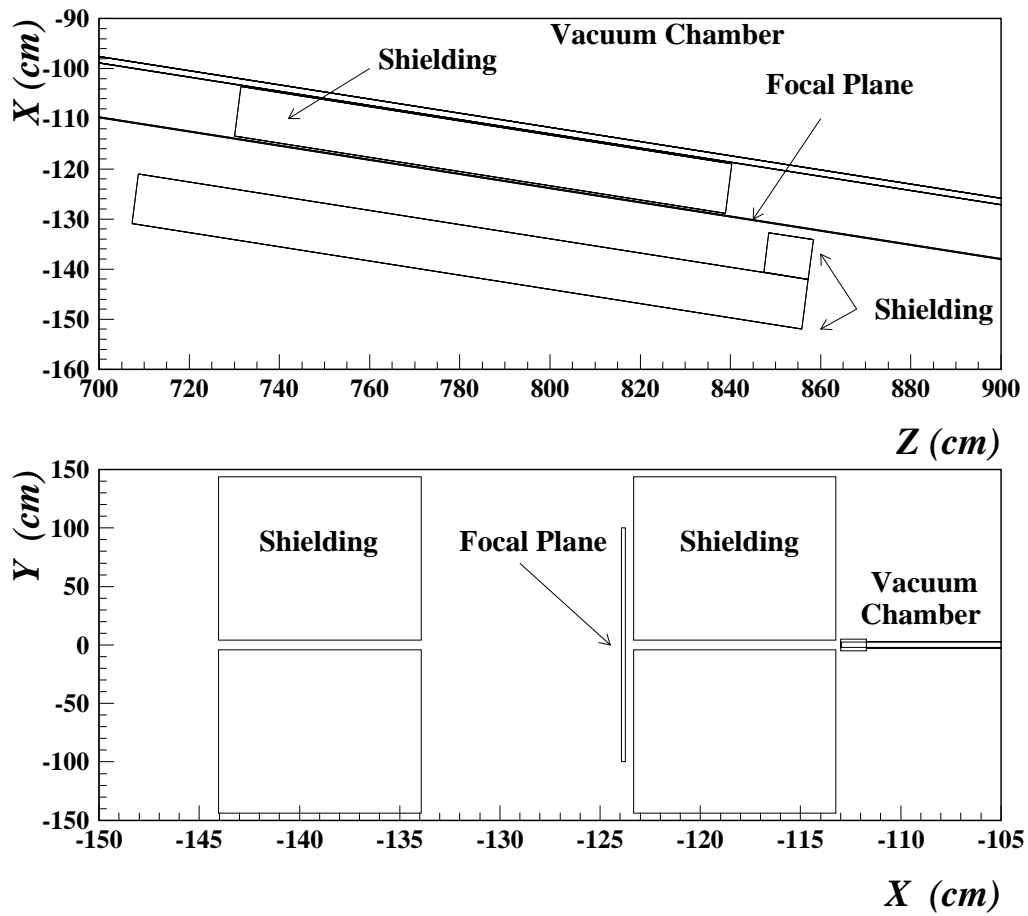
Figure 4: Geant geometry of the microscope detector area shielded with polyethylene walls, geometry #6: Elevation view (top), side view corresponding to the cut perpendicular to the z-axis at z = 800 cm (bottom).
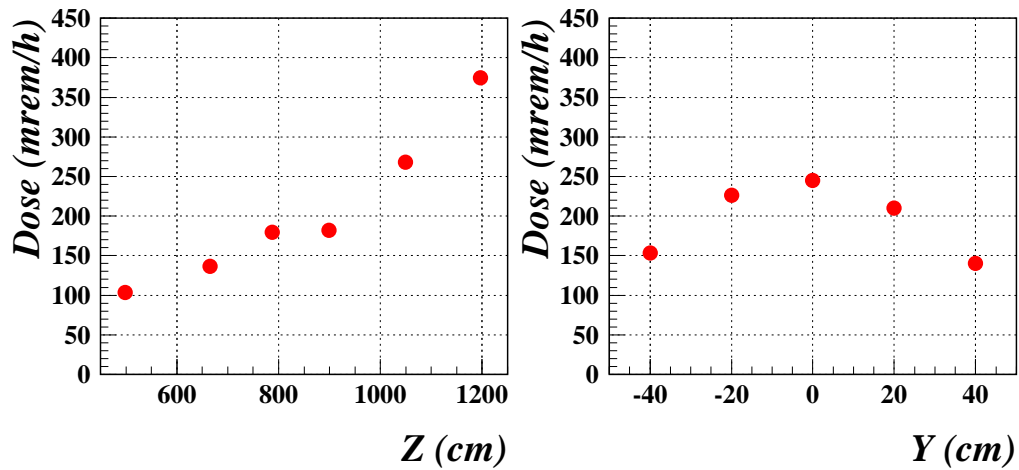
Figure 5: Neutron dose distribution along the focal plane corresponding to the geometry with the long vacuum chamber and 6″ beam pipe, geometry #5 (left). Neutron dose distribution as a function of Y coordinate for the microscope detector region (right).
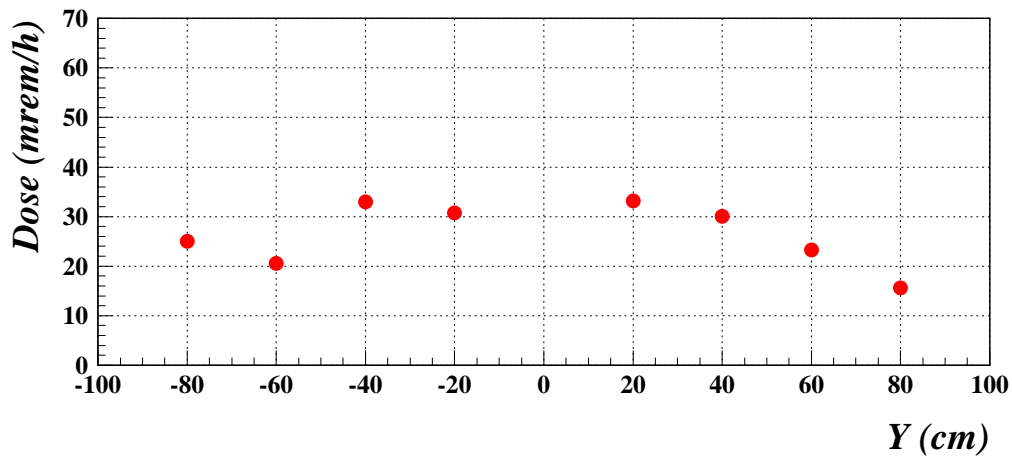

Figure 6: Neutron dose distribution in the microscope detector area as a function of Y coordinate for the geometry with polyethylene shielding, geometry #6.
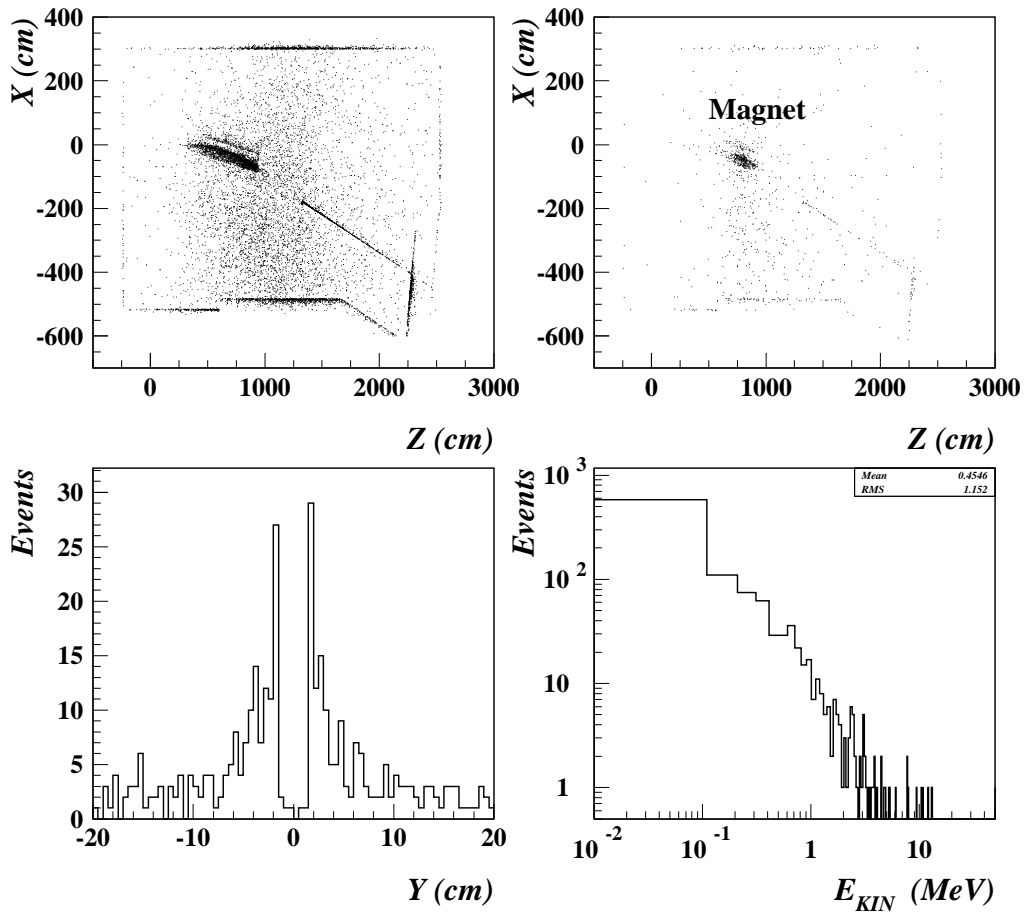
Figure 7: Z-X coordinate of the origin of neutrons which pass through the focal plane (top left) and through the microscope detector region (top right). Y coordinate of the origin of neutrons inside the magnet (bottom left). Energy distribution of neutrons that pass through the microscope detector region (bottom right).
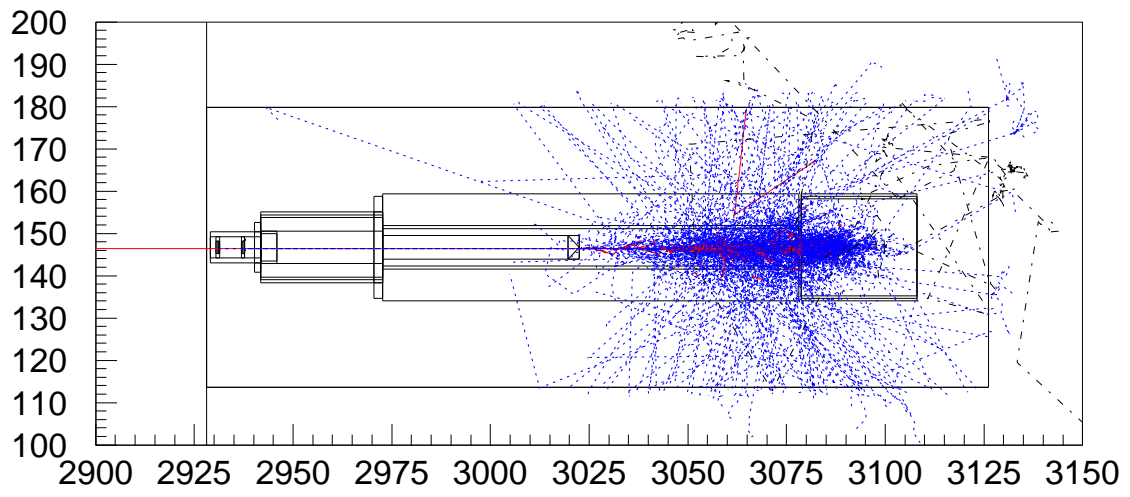
Figure 8: Interactions inside the beam dump induced by a 12 GeV electron.